

# Hybrid deep convolution model for lung cancer detection with transfer learning

Sugandha Saxena<sup>1</sup>, S. N. Prasad<sup>2</sup>, Ashwin M Polnaya<sup>3</sup>, Shweta Agarwala<sup>4\*</sup>

<sup>1</sup>*School of Electronics and Communication Engineering, REVA University Bangalore, India*

<sup>2</sup>*Department of Electronics and Communication Engineering, Manipal Institute of Technology Bengaluru, Manipal Academy of Higher Education, Manipal, Bengaluru, India*

<sup>3</sup>*Department of Radiology, Interventional Radiology Division, A J Hospital & Research Centre, Kuntikana, Mangalore, India*

<sup>4</sup>*Department of Electrical and Computer Engineering, Aarhus University, Aarhus 8200, Denmark*

*\*corresponding author: shweta@ece.au.dk*

**Abstract:** Advances in healthcare research have significantly enhanced our understanding of disease mechanisms, diagnostic precision, and therapeutic options. Yet, lung cancer remains one of the leading causes of cancer-related mortality worldwide due to challenges in early and accurate diagnosis. While current lung cancer detection models show promise, there is considerable potential for further improving the accuracy for timely intervention. To address this challenge, we introduce a hybrid deep convolution model leveraging transfer learning, named the Maximum Sensitivity Neural Network (MSNN). MSNN is designed to improve the precision of lung cancer detection by refining sensitivity and specificity. This model has surpassed existing deep learning approaches through experimental validation, achieving an accuracy of 98% and a sensitivity of 97%. By overlaying sensitivity maps onto lung Computed Tomography (CT) scans, it enables the visualization of regions most indicative of malignant or benign classifications. This innovative method demonstrates exceptional performance in distinguishing lung cancer with minimal false positives, thereby enhancing the accuracy of medical diagnoses.

## 1. Introduction

Accurately detecting diseases remains a significant challenge in the realm of medical research. Among various cancer types, lung cancer is particularly perilous due to its high mortality rate and substantial health impacts [1]-[3]. According to data from India's National Cancer Registry Program, approximately 784,821 individuals die from cancer each year [4]-[5]. Neoplasms, which are characterized by abnormal cell growth, can develop into benign or malignant tumors and nodules in the lungs. Timely detection of lung or pulmonary nodules is essential for improving treatment outcomes and increasing patient survival rate.

Computed Tomography (CT) scans have become the primary diagnostic technique for detecting lung cancer. These scans offer high resolution, minimal distortion, and enhanced contrast, which allow for detailed examination of the lungs and quicker detection of lung nodules [6]. However, noise in CT scan images can compromise image clarity, posing challenges for radiologists in identifying early-stage lung cancer. To overcome these challenges, deep neural network-based models have been developed, significantly improving the accuracy of cancer detection [7].

In recent years, deep learning, a subset of artificial intelligence (AI), has shown tremendous promise in various medical imaging applications. Deep learning has the ability to automatically learn and extract features from large datasets, making it a powerful tool for image analysis and pattern recognition [8],[9]. This technology has revolutionized medical imaging by providing enhanced precision and reliable diagnostic tools, ultimately enhancing early detection and intervention of diseases like lung cancer [10],[11]. Lakshmanaprabu et al. [12] developed a deep learning model with 94.56% accuracy for categorizing lung CT images as malignant or noncancerous using an Optimal Deep Neural Network (ODNN) and LDA. They used a modified gravitational search algorithm (MGSA) to optimize the ODNN. Lu Y et al. [13] created a CNN model that, when paired with machine learning techniques like Naive Bayes, SVM, and Decision Tree, together with nodule segmentation networks like VGG 16 and Dilated Convolution, achieved 88% accuracy in lung cancer detection. Sannasi Chakravarthy and Rajaguru [14] employed Grey Level Co-occurrence and the Chaotic Crow Search Algorithm (CCSA) by using XGBoost and random forest classifiers along with a preprocessing pipeline containing UNet and ResNet models. Bhatia et al. [15] were able to achieve 84% greater

accuracy than they could have with conventional approaches. To segregate lung cancer in X-ray images, Joon et al. [16] employed an active spline model. They also used SVM classification, K-means and fuzzy C-means clustering for feature extraction. Using an ANN model and a dataset of 83 CT images, another study used image processing and machine learning techniques including KNN and RF to classify lung cancer and produced accurate predictions [17]. Leveraging this technology, we propose a novel deep learning model called MSNN as it is designed specifically for detecting lung cancer from medical images. The model is termed "hybrid" because it synergistically combines multiple techniques to enhance its performance in lung cancer detection. It integrates a deep convolutional neural network (CNN) framework, which excels at learning intricate patterns from 512x512 grayscale lung CT scan images. Additionally, it employs transfer learning by leveraging pre-trained networks such as AlexNet, allowing the model to utilize pre-existing knowledge and improve. Furthermore, the extracted deep features are fed into a K-Nearest Neighbor (KNN) classifier for the final classification, effectively combining the strengths of CNNs in feature extraction and KNN in classification. This amalgamation of methodologies ensures superior accuracy and sensitivity, making it a robust tool for lung cancer detection.

There are many noteworthy aspects of this model. Firstly, the model uses pre-batch normalization and max pooling layers, strategically employed to reduce model complexity. Secondly, Visualization of sensitivity maps aids in understanding which areas of an image contribute significantly to its classification. Thirdly, the model can identify different shapes of nodules in lung CT scan image. Fourthly, the global average pooling layer (GAP) has been used to overcome the issue of overfitting by reducing the number of parameters. Lastly, the model supports multiple splits of dataset as training and testing for assessing its performance more robustly by training and evaluating on different subsets of the data.

## 2. Methodology

This research utilizes a comprehensive database of lung CT scan images sourced from a private hospital, encompassing a diverse array of cases. The primary objective is to develop a novel convolutional neural network (CNN) framework to accurately identify lung cancer in these scans. The proposed Maximum Sensitivity Neural Network (MSNN) is an advanced architecture meticulously crafted to differentiate between cancerous and noncancerous lung CT images. The innovative MSNN architecture is constructed based on foundational principles from the pre-existing deep neural network, AlexNet [21].

Each CT scan image serves as an input to the MSNN model, which performs an extensive analysis to classify it as either cancerous or noncancerous. The output is not merely a binary label but also includes a probability score associated with the predicted classification, providing clinicians and researchers with additional insights to enhance the interpretability and utility of the MSNN model in lung cancer diagnosis.

AlexNet, a renowned deep convolutional neural network (CNN) structure, is known for its efficacy in image classification tasks, including lung cancer detection. However, its extensive depth and significant parameter count make it susceptible to overfitting, especially when dealing with limited datasets. AlexNet's architecture features five convolutional layers, three max-pooling layers, three fully connected layers, and a SoftMax layer for final output classification.

The MSNN model has been proposed to address the potential overfitting challenges faced by deep learning models. This model integrates a Global Average Pooling (GAP) layer within its design. The overall flow and architecture of proposed model (figure 1) comprises of five sequential blocks. Blocks 1 to 4 each consist of four layers: convolution (conv), Batch Normalization (BN), Rectified Linear Unit (ReLU), and a max-pooling layer. Block 5 includes a convolutional layer, Batch Normalization, ReLU, a Global Average Pooling (GAP) layer, followed by a fully connected layer and a SoftMax layer. These layers process grayscale images sized at 512x512 pixels, facilitating image classification tasks. The model begins with an input layer that processes 512x512 grayscale CT scan images, followed by a series of convolutional layers (Conv) paired with batch normalization (BN) and rectified linear unit (ReLU) activation layers, which are designed to extract detailed features. Max-pooling layers reduce dimensionality, preserving essential features while minimizing computation. A Global Average Pooling (GAP) layer then condenses spatial information from feature maps into a 1-dimensional vector, enhancing generalization and reducing overfitting risk. The final fully connected (FC) layer and SoftMax (SM) layer classify the image as cancerous or non-cancerous. This architecture

effectively integrates convolutional feature extraction with K-Nearest Neighbor (KNN) classification for enhanced accuracy and interpretability in lung cancer detection.

The training of the MSNN model involves two main steps: first, distinguishing between malignant and noncancerous lung lesions using CT scan images, and second, extracting features from the deep layers of these images. These features are then input into a K-Nearest Neighbors (KNN) classifier for further classification. Although CNNs are adept at image classification, medical applications often require complex classification where class differences are subtle. Therefore, a supplementary KNN classifier refines the classification process to achieve more precise outcomes. The combination of MSNN and KNN architectures has been meticulously engineered. Initially, preprocessed grayscale CT scan images pass through a series of convolutional, batch normalization, ReLU, and max-pooling layers across blocks 1 to 5. These convolutional layers use various filters to capture a wide range of features, from edges to intricate patterns. After feature extraction by the global average pooling layer, the layer computes average values from the feature maps, resulting in a condensed 1-dimensional vector. This vector is then input to the fully connected layer, where each neuron applies weights to the input values, incorporates bias terms, and calculates a weighted sum. The final sum is directed to the SoftMax layer, which generates class probabilities. Post-feature extraction by the MSNN, the features from the fully connected layer can be seamlessly integrated into the KNN classifier for further analysis.

The effectiveness of the KNN classification method depends on the choice of the parameter  $k$ . In this research, the optimal  $k$  value for the KNN classifier was determined using the elbow method. This technique involves plotting the sum of squared error (SSE) values against different  $k$  values and identifying the point on the graph where increasing  $k$  no longer significantly affects the SSE. This turning point, known as the "elbow," signifies the optimal  $k$  value, which was found to be 3 in this study.

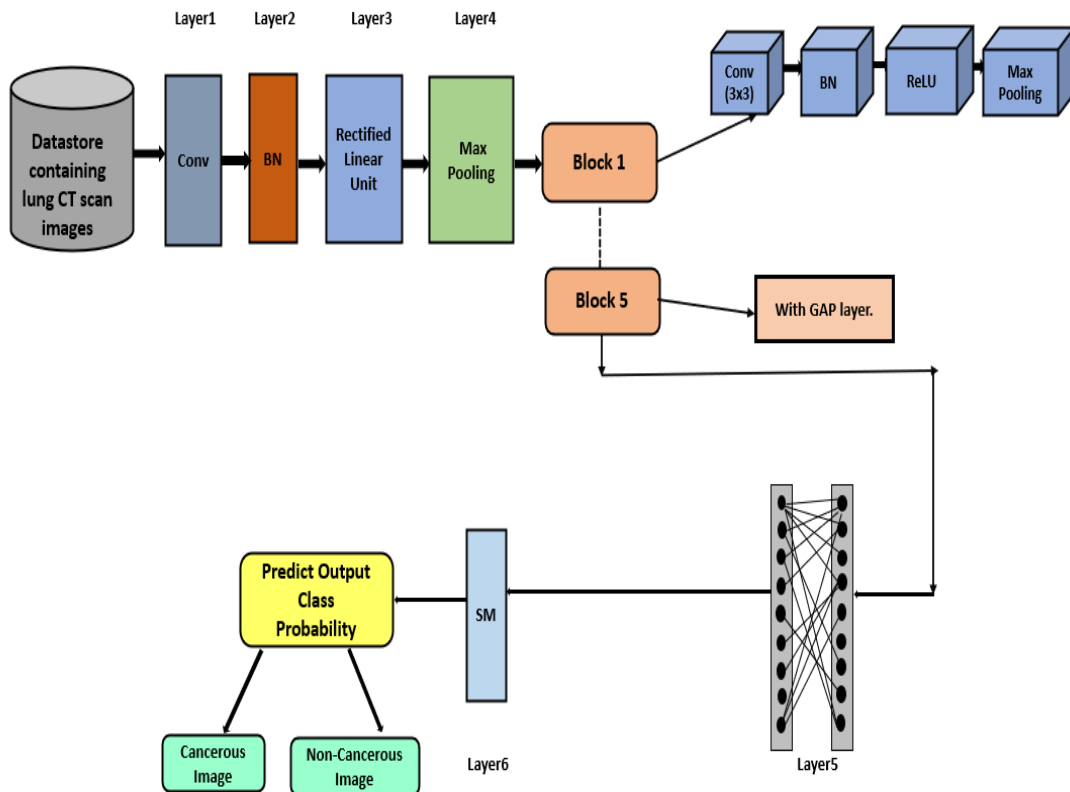


Figure 1: The overall flow of the proposed Maximum Sensitivity Neural Network (MSNN) model for lung cancer detection, illustrating the structure and functionality of each layer.

### 3. Experimental Results

The efficacy of MSNN has been demonstrated by several trials and comparisons with other models utilizing datasets of CT images from the lungs.

#### 3.1 Dataset and training options:

The successful classification of test images relies on numerous parameters, making the training of the neural network a pivotal aspect that demands meticulous consideration. The subsequent configuration has been established for the training of MSNN. The ADAM optimization method has been opted for, which iteratively updates the learning coefficients. It independently manages learning rates for each parameter and dynamically adapts these rates during training, thus requiring minimal manual tuning of hyperparameters. The training is conducted with a batch size of 20 and an epoch value of 20 for MSNN. This selection of optimal batch size and epoch value is the outcome of systematic trial and error. The batch size plays a crucial role in balancing the network's convergence rate and accurate estimation [22]. Nevertheless, an excessively large batch size was avoided due to potential time consumption and memory utilization. It's noted that an overly high epoch value may lead to overfitting, while an insufficient epoch value may result in early convergence and termination of training.

For this work, lung CT scan images in DICOM format were sourced from A.J Hospital and Research Centre for the assessment of MSNN performance. The dataset encompasses 434 lung CT scan images, comprising 249 images from patients with lung cancer and 185 images from patients with healthy lungs.

Figure 2 displays several samples of lung CT scan images from the dataset. Images (a), (c), and (e) show cancerous nodules marked by green arrows, while images (b), (d), and (f) are non-cancerous and free of any suspicious nodules. Each image in the dataset is reviewed with the help of a radiologist to manually identify the nodules. The MSNN architecture employs different layers with distinct functions, detailed as follows:

1. Input layer-The MSNN architecture accepts grayscale CT scan images.
2. Convolution Layer- In this layer, convolution is performed between the filter size (g) and the input image (f) using equation (1) [23].

$$f(x) * g(x) = \sum_{k=-\infty}^{\infty} f(k) \cdot g(x - k) \quad (1)$$

where x and k are spatial variables.

A smaller filter size may cause an overfitting issue, and a bigger filter size may make underfitting worse. Therefore, this layer makes use of eight filters, each of 6x6 size.

3. Batch Normalization- The next layer is called the Batch Normalisation (BN) layer, which speeds up training and lessens network sensitivity. For the 'i' unit, normalization is carried out as follows over a batch (v) of m instances using equation (2); each instance corresponds to a single image in the dataset along with its accompanying label.

$$\mu_i = \sum_{r=1}^m v_i^r / m \quad (2)$$

Where r ranges from 1 to m

Secondly, compute batch variance [23] by using below equation (3):

$$\sigma_i^2 = \sum_{r=1}^m (v_i^r - \mu_i)^2 / m \quad (3)$$

Thirdly, compute normalized batch instances [23] by using equation (4):

$$v_n^r = v_i^r - \mu_i / \sigma_i \quad (4)$$

Lastly, scale with learnable parameters  $\gamma_i$  and  $\beta_i$  [23] by using equation (5):

$$a_i^r = \gamma_i * v_n^r + \beta_i \quad (5)$$

4. ReLU (Rectified Linear Unit) layer-It helps to add nonlinearity to the network by adding a rectifier function which is computing linear operations during convolution [24]. The function works by using equation (6):

$$f(x) = 0, x < 0$$

$$f(x) = x, x > 0 \quad (6)$$

5. Max pooling layer- Reducing the size of the convolved feature map aids in cutting down on computational expenses.
6. Global Average pooling (GAP) layer- Applying this layer to the feature maps summarizes the spatial information within each channel by taking the average value across all spatial locations. This operation retains the channel-wise information while discarding the spatial dimensions, resulting in a compressed representation of the feature maps.
7. Fully Connected (FC) Layer- It helps in classifying the images.
8. Soft Max (SM)layer- It creates a probability distribution from the last layers output.

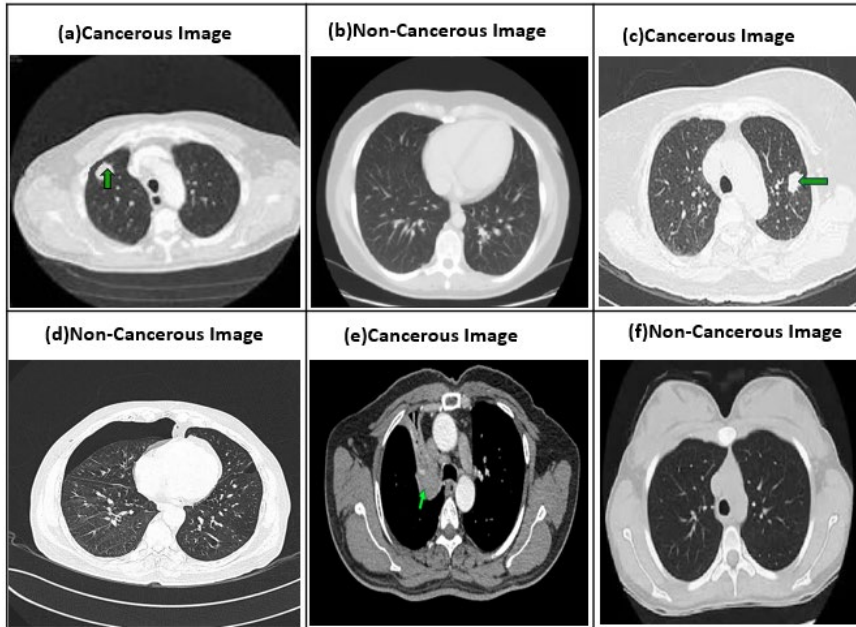


Figure 2. Representative samples of lung CT scan images from the study's database showcasing both cancerous and non-cancerous cases.

### 3.2 Performance Metrics:

MSNN performance has been evaluated by measuring accuracy[25], precision, sensitivity, specificity, and F-score[26]. True positive (TP), false positive (FP), true negative (TN), and false negative (FN) values were derived from the confusion matrix. Accuracy =  $\frac{TN+TP}{TN+TP+FN+FP}$  (7)

$$\text{Precision} = \frac{TP}{TP+FP} \quad (8)$$

$$\text{Recall} = \frac{TP}{TP+FN} \quad (9)$$

$$\text{F-Score} = \frac{2 * (\text{Precision} * \text{Recall})}{\text{Precision} + \text{Recall}} \quad (10)$$

$$\text{Specificity} = \frac{TN}{TN+FP} \quad (11)$$

Figure 3 represents the training and validation progress of a model over 300 iterations. With respect to accuracy plot (top plot), the x-axis shows the number of iterations, ranging from 1 to 300 and y-axis shows the accuracy of model ranging from 0% to 100%. The light blue line represents the training accuracy and dark blue line represents smoothed version of the training accuracy on training dataset whereas black dots represent the accuracy of model on validation dataset. Similarly, with respect to loss plot (bottom plot), the x-axis shows the number of iterations ranging from 1 to 300 and y-axis indicates the loss value which ideally decreases as training progresses. The orange line represents the training loss and dark orange line represents the smoothed version of the training loss on the training dataset wherein the black dots represent the loss on the validation dataset.

Figure 4 displays confusion matrix for different splits of dataset. The dataset is divided into training and validation sets through random allocation for split1, where 70% of the images are employed for training, while the remaining 30% are designated for testing. Similarly, split2, split3, and split4 entail 75%, 80%, and 85% of the dataset images for training, respectively, leaving the remainder for testing. Consequently, the training procedure is executed four times, each with distinct dataset splits. This approach gauges the model's performance across various training scenarios and bolsters a more robust assessment of its generalization capabilities. In figure 5, the Y-axis of the graphs displays the loss function (minimal goal), while the X-axis displays the quantity of function evaluations. The function evaluation shows how many times the algorithm has been run during validation, whereas the loss function calculates the difference between a model's predicted and actual values. In this case, the suggested MSNN model and the Support Vector Machine (SVM) both employ the Mean Square Error (MSE) as their loss function. The graphs show how the number of function evaluations affects the MSE. The loss function (blue curve) of the SVM model starts higher and falls off more gradually. It seems that the SVM's minimal observed objective levels off at an MSE of around 0.04. The proposed MSNN model's loss function (green curve) starts at a similar value but decreases more rapidly and stabilizes at a much lower MSE, approximately 0.01. The significant reduction in the loss function for the MSNN model, reaching around 0.01 compared to the SVM's 0.04, highlights the superior performance of the MSNN model. This lower loss function translates to an accuracy of 96.9% and a sensitivity of 94.6% for the MSNN model, making it particularly effective for lung cancer detection, especially when compared to the typically lower accuracies reported in previous studies [32].

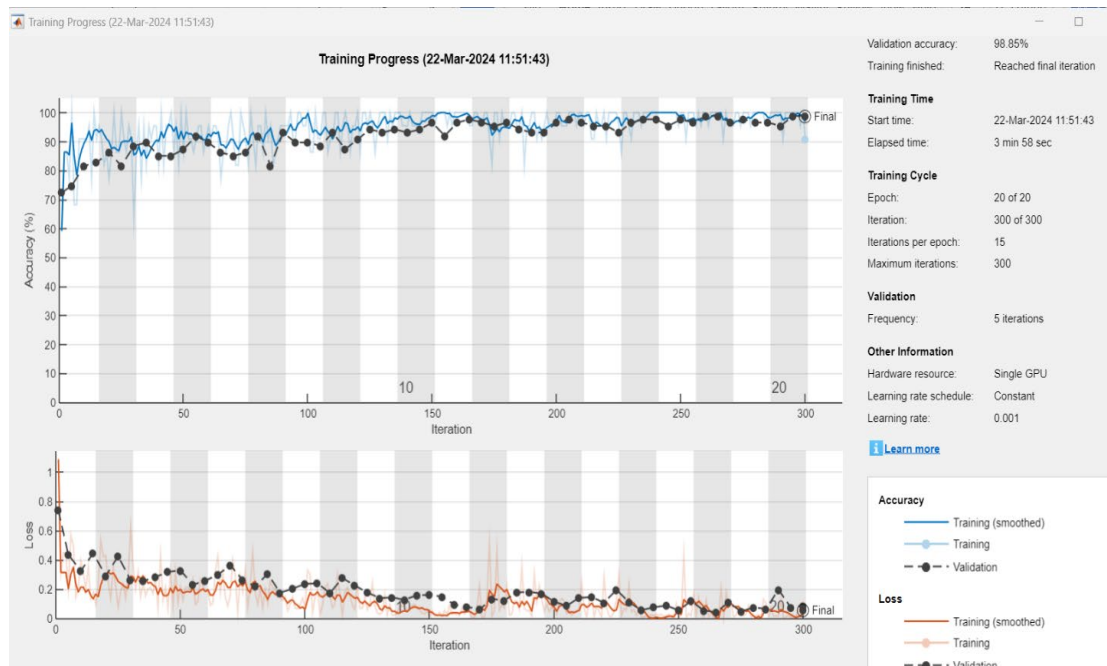


Figure 3. Accuracy and loss plots illustrating the training and validation performance of the Maximum Sensitivity Neural Network (MSNN) model.

#### 4. Discussion

Table I represents the architecture details of proposed models. Table II compares performance metrics across split1, split2, split3, and split4. It's evident that split 2 exhibits the highest accuracy, precision, recall, specificity, and F-score attributes because the percentage of training data in Split 2 effectively captures the underlying patterns in the dataset. The performance metrics across four data splits (Split1 to Split4) for the Maximum Sensitivity Neural Network (MSNN) reveal interesting insights into the model's efficacy and generalizability. This balance provides the model with enough samples to ensure good generalization without overfitting. Notably, the false positive rate (FPR) is at 0% in split 2, indicating the model's adeptness in distinguishing between positive and negative cases, reducing the misclassification of negatives as positives.

Performance comparison of Proposed MSNN with other existing deep learning models has been shown in Table III.

From the results it can be observed that MSNN achieved an accuracy of 98% and sensitivity of 97%. Therefore, it can be concluded that MSNN worked well in the identification of lung cancer because the accuracy reported in [27],[28] is 93%, and 96% respectively. To ensure fair comparison similar datasets are utilized in [27],[28] which are acquired from private hospitals consisting of lung CT scan images of size 512x512.

Typically, medical data is so big that deep neural networks constantly struggle with overfitting. An average pooling layer, which lowers network complexity, is utilized to solve this issue. Accuracy and loss plots clearly indicate that the proposed model does not overfit the data and therefore exhibits good efficacy. The trade-off between the true positive rate and the false positive rate is shown in figure 6.

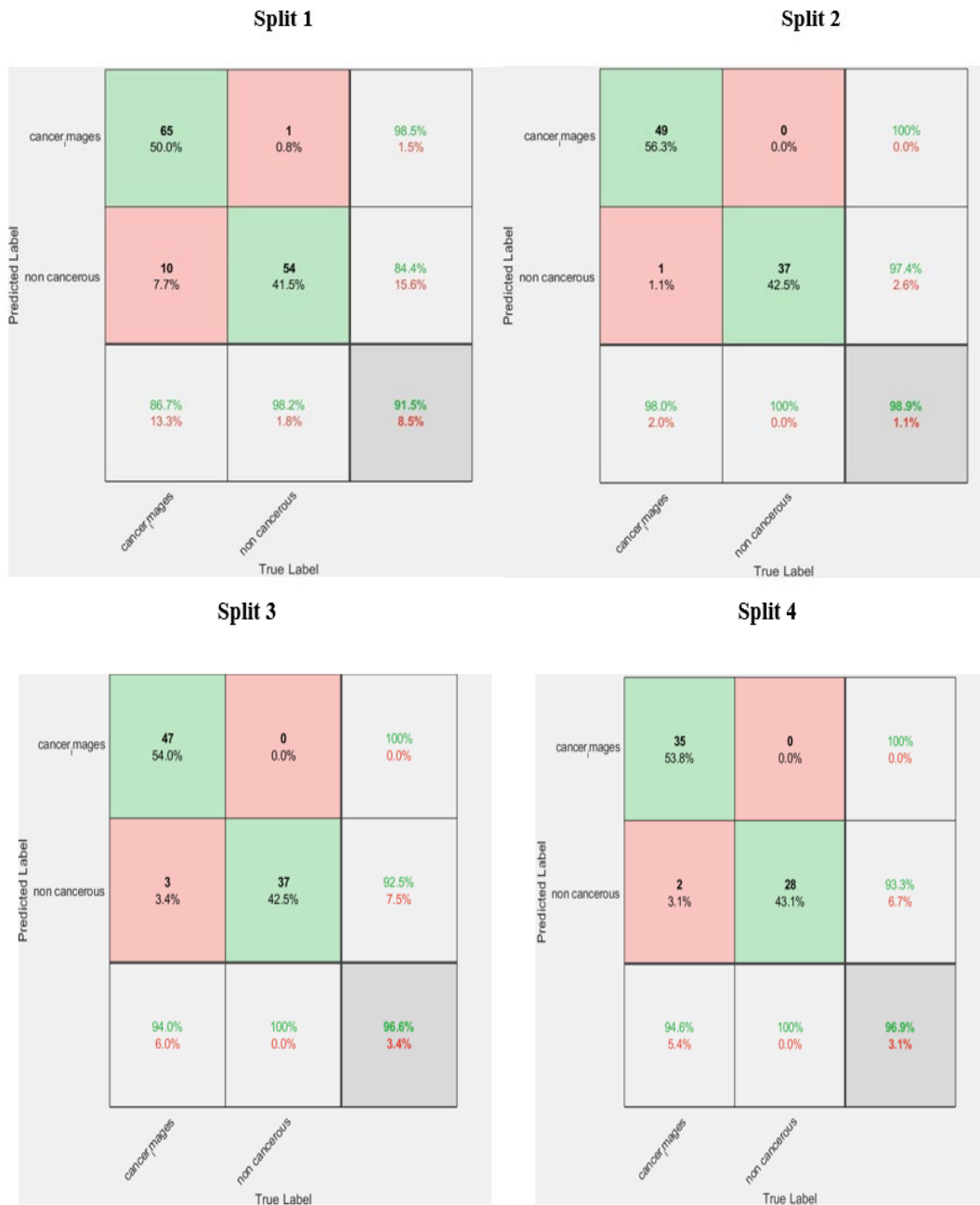


Figure 4. Confusion matrix illustrating the performance of the MSNN model on binary classification of lung CT images across different dataset splits: Split1, Split2, Split3, and Split4.

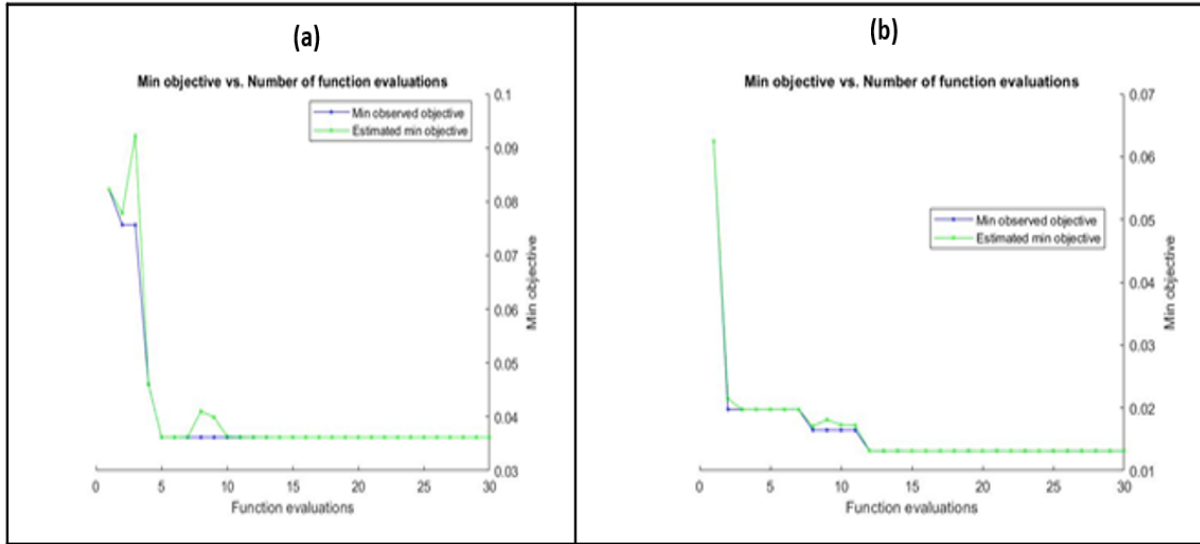


Figure 5. Plot of loss function versus function evaluation using (a) SVM classifier (c) the proposed MSNN classifier.

TABLE I: Detailed architecture of the Maximum Sensitivity Neural Network (MSNN) model, outlining each layer's parameters and function in the lung cancer detection process.

Type of Layer	Output shape	Number of Filters	Filter size	Stride	Padding	Padding type	Pool size	Parameters Used
Conv	[512,512,8]	8	[6 6]	[1 1]	[0 0 0 0]	Same	-	296
BN	[512,512,8]	-	-	-	-	-	-	32
ReLU	[512,512,8]	-	-	-	-	-	-	0
Max Pooling	[256,256,8]	-	-	[2 2]	[0 0 0 0]	Manual	[2 2]	0
Conv	[256,256,16]	16	[3 3]	[1 1]	[0 0 0 0]	Same	-	1168
BN	[256,256,16]	-	-	-	-	-	-	32
ReLU	[256,256,16]	-	-	-	-	-	-	0
Max pooling	[128,128,16]	-	-	[2 2]	[0 0 0 0]	Manual	[2 2]	0
Conv	[128,128,32]	32	[3 3]	[1 1]	[0 0 0 0]	Same	-	4640
BN	[128,128,32]	-	-	-	-	-	-	128
ReLU	[128,128,32]	-	-	-	-	-	-	0
Max pooling	[64,64,32]	-	-	[2 2]	[0 0 0 0]	Manual	[2 2]	0
Conv	[64,64,64]	64	[3 3]	[1 1]	[0 0 0 0]	Same	-	18496
BN	[64,64,64]	-	-	-	-	-	-	256
ReLU	[64,64,64]	-	-	-	-	-	-	0
Max pooling	[32,32,64]	-	-	[2 2]	[0 0 0 0]	Manual	[2 2]	0
Conv	[32,32,128]	128	[3 3]	[1 1]	[0 0 0 0]	Same	-	73856
BN	[32,32,128]	-	-	-	-	-	-	512
ReLU	[32,32,128]	-	-	-	-	-	-	0
Max pooling	[16,16,128]	-	-	[2 2]	[0 0 0 0]	Manual	[2 2]	0
Conv	[16,16,256]	256	[3 3]	[1 1]	[0 0 0 0]	Same	-	295168
BN	[16,16,256]	-	-	-	-	-	-	0
ReLU	[16,16,256]	-	-	-	-	-	-	0
GAP	[1,1,256]	-	-	-	-	-	-	0
FC	[1,1,512]	-	-	-	-	-	-	131584
BN	[1,1,512]	-	-	-	-	-	-	0
ReLU	[1,1,512]	-	-	-	-	-	-	0

FC	[1,1,2]	-	-	-	-	-	-	1026
SM	[1,1,2]	-	-	-	-	-	-	0

TABLE II: Comparison of performance parameters for different splits of dataset.

Splits	Accuracy	Sensitivity	Precision	F-Score	Specificity
<i>Split1</i>	91%	84%	98%	90%	98%
<i>Split2</i>	98%	97%	99%	98%	99%
<i>Split3</i>	96%	92%	99%	96%	99%
<i>Split4</i>	96%	93%	99%	96%	99.9%

TABLE III: Performance comparison of proposed model with other existing deep learning models.

Deep Learning Models	Accuracy (%)	Sensitivity (%)	Precision (%)
CNN Model with SVM classifier[27]	93	85	73
DL based Classification[28]	96	93	96
MSNN (Proposed Method[29])	98	97	99

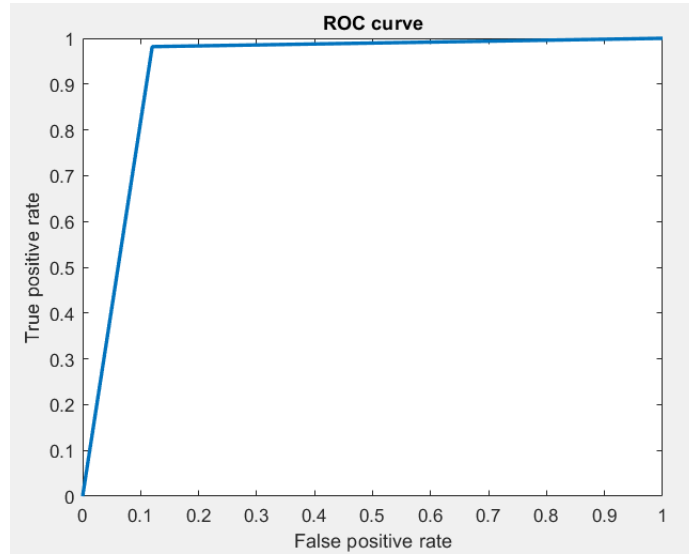


Figure 6. The ROC curve of the proposed model using private dataset.

Sensitivity maps [29],[30] have been used in this work to determine which area of the CT scan image contributes the most to the proposed model classification. It is clear from these maps that the classification decision is based on a deep neural network image feature. Sensitivity maps use a mask, which is a grey square, to cover different portions of the input image to calculate the change in probability score for a specific test image. Figure 7. shows lung CT scan image with a probability score and sensitivity maps overlaid on it. Red area in sensitivity maps shows highest contribution in classification decision wherein blue area in maps represents less or no contributions in classification decision.

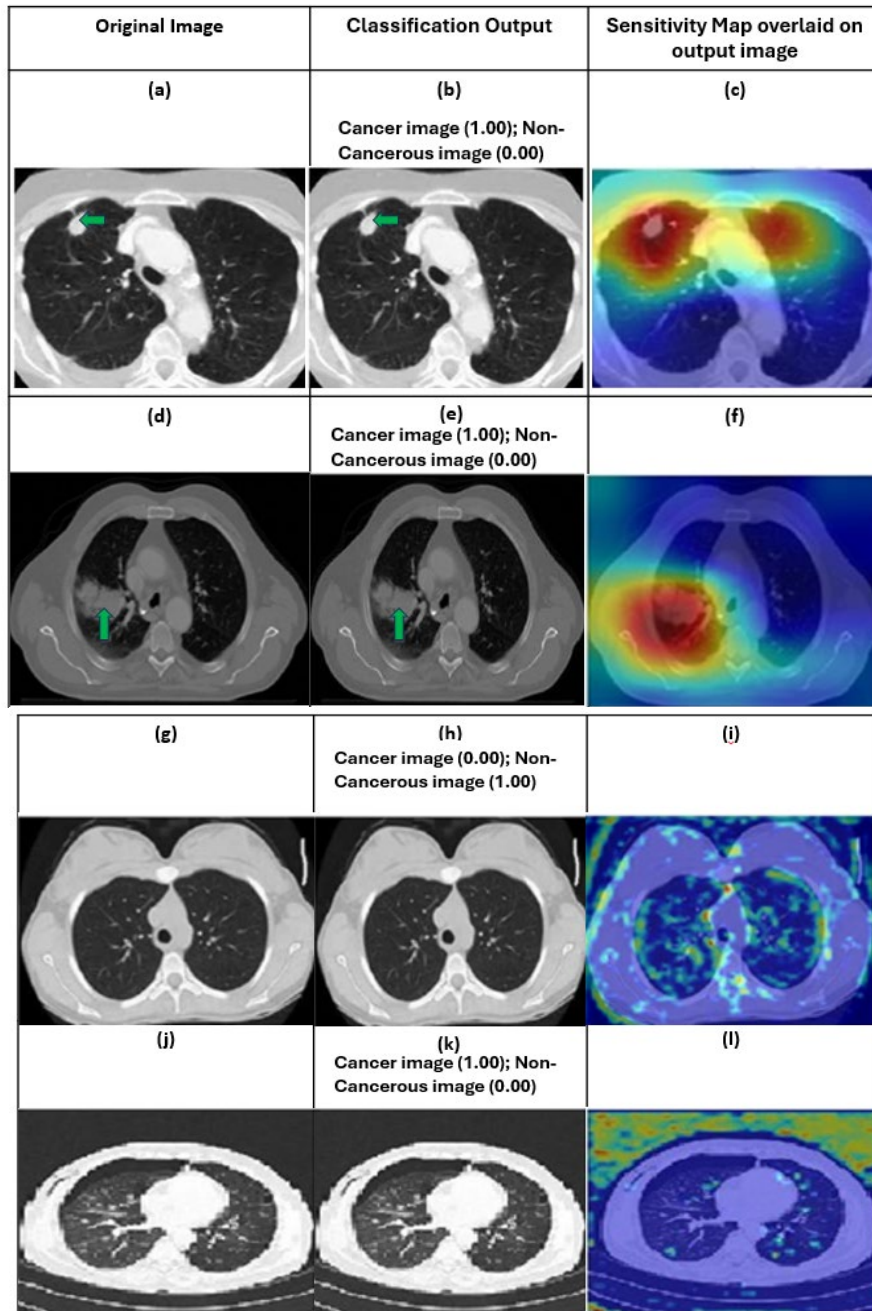


Fig. 7. MSNN Model classifying lung cancer with a probability score and plotting of Sensitivity Map.

The proposed model in this research successfully extracts deep-layer features that contain crucial information about the images. Figure 8 illustrates the feature extraction process of the Maximum Sensitivity Neural Network (MSNN) model, focusing on the weights and features at different convolutional layers. Figure 8(a) represents the filters (weights) used in the first convolutional layer of the MSNN model. These filters detect basic features like edges and textures in the input images. Figure 8(b) displays the feature maps generated after applying the first convolutional layer filters to the input images, highlighting edges and simple patterns detected in the input images. Figure 8(c) shows the filters used in the third convolutional layer. As the network deepens, the filters become more complex, enabling the detection of more intricate patterns. Figure 8(d) illustrates the feature maps produced after applying the third convolutional layer filters, capturing more detailed patterns and structures in the input images. Figure 8(e) depicts the filters used in the fifth convolutional layer. The deeper layers of the network capture even more complex and abstract features. Finally, Figure 8(f) displays the feature maps generated after applying the fifth convolutional layer filters. At this stage, the feature

maps contain high-level abstract features that are critical for distinguishing between cancerous and non-cancerous regions in lung CT scans. The results indicate that deeper layers, by combining earlier data, can extract more abstract and higher-level information. Consequently, features derived from lower levels are more suitable for classification tasks [31]. Once extracted, these features are fed into a K-Nearest Neighbour (KNN) classifier. However, using the classifier requires numerous parameters to be manually adjusted. The suggested MSNN model represents a deep convolutional neural network designed specifically for identifying lung cancer. However, when dealing with a sizable dataset, there's always a risk of overfitting and therefore the model's ability to accurately classify test data may be compromised. To address this issue, this work employs the Global Average Pooling layer, which serves to enhance model performance by minimizing the loss function value. A reduced loss function implies improved accuracy in predictions.

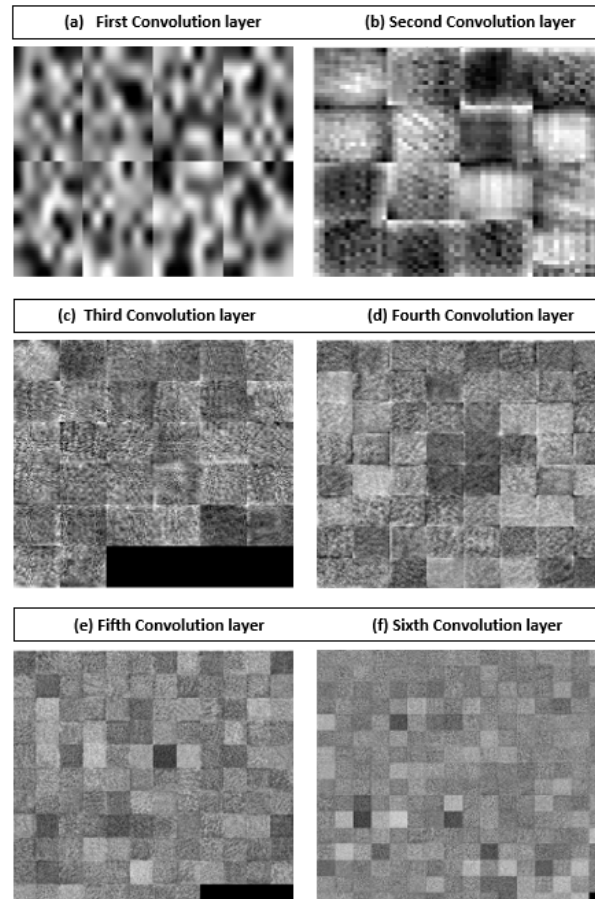


Figure 8: Visualization of features extracted from different convolutional layers of the proposed Maximum Sensitivity Neural Network (MSNN) model. Each subfigure represents the output of a specific convolutional layer, showcasing the progressive complexity of feature extraction throughout the network.

## 5. Conclusion

High accuracy is essential, while building a deep learning model for lung cancer diagnosis. As a result, MSNN model with rigorous design has been proposed which gives impressive levels of efficiency. In comparison to previous methods, the proposed model outperformed them with accuracy of 98% and sensitivity of 97%. The suggested model considerably aids in the classification process by successfully extracting features from multiple convolution layers. On the input lung CT scan image, a sensitivity map has been created, showing the nodule area in red. This map makes it easier to distinguish between cancerous and non-cancerous areas of the image. Future work will mostly focus on resolving specific aspects that often need to be adjusted manually

to obtain high accuracy with a classifier. Fixing this problem could be a major goal of future projects. One possible option is to use Bayesian optimization, which is a method for automatically choosing the best

parameters. This strategy would improve the effectiveness of the classifier and expedite the parameter selection procedure.

### Data Availability

In this work, lung CT scan images has been collected from 434 cancer patients from A.J. Institute of Medical Sciences in Mangalore, India. Data available on request from the authors.

### Conflicts of Interest

The authors declare that they have no conflicts of interests.

### Acknowledgements

The authors express their gratitude to the Department of Radio-Diagnosis at the Interventional Radiology Division of the A.J. Institute of Medical Sciences in Mangalore, India. Their assistance in obtaining patient database from the hospital and guidance in comprehending raw medical pictures is greatly appreciated. The authors would like to thank REVA University for providing the facilities needed to conduct the research.

### References

- [1] R. L. Siegel, K. D. Miller, H. E. Fuchs, and A. Jemal, Cancer statistics, 2022, *CA: A Cancer Journal for Clinicians*, vol. 72, no. 1, pp. 7–33, Jan. 2022, doi: 10.3322/CAAC.21708
- [2] Rui Li, Chuda Xiao, Yongzhi Huang, Haseeb Hassan and Bingding Huang, Deep Learning Applications in Computed Tomography Images for Pulmonary Nodule Detection and Diagnosis: A Review, *Diagnostics*, vol. 12, pp. 1-21, 2022.
- [3] Kumar, Y., Gupta, S., Singla, R., & Hu, Y. C, A systematic review of artificial intelligence techniques in cancer prediction and diagnosis, *Archives of Computational Methods in Engineering*, pp. 1-28, 2021.
- [4] P. Mathur et al., Cancer Statistics, 2020: Report from National Cancer Registry Programme, India, *JCO Global Oncology*, vol. 6, no. 6, pp. 1063–1075, Nov. 2020, doi: 10.1200/GO.20.00122.
- [5] Hyuna Sung, Jacques Ferlay, Rebecca L. Siegel, Mathieu Laversanne, Isabelle Soerjomatara, Ahmedin Jemal DMV, Global Cancer Statistics 2020: GLOBOCAN Estimates of Incidence and Mortality Worldwide for 36 Cancers in 185 Countries, *CA: A cancer journal for clinicians*, Vol 7, Issue 3, pp.209-249, 2021.
- [6] Sharmila Nageswaran, G. Arunkumar, Anil Kumar Bisht, Shivlal Mewada, J. N. V. R. Swarup Kumar, Malik Jawarneh, and Evans Asenso, Lung Cancer Classification and Prediction Using Machine Learning and Image Processing, *Hindwai*, pp. 1-6,2022.
- [7] Gould M. K, Huang B. Z, Tammemagi M. C, Kinar Y, and Shiff R, Machine learning for early lung cancer identification using routine clinical and laboratory data, *American Journal of Respiratory and Critical Care Medicine*, Vol: 204, issue no.4, 445-453,2021.
- [8] Wang X, Wang L, and Zheng P, SC-Dynamic R-CNN: A Sel Calibrated Dynamic R-CNN Model for Lung Cancer Lesion Detection, *Computational and Mathematical Methods in Medicine*, pp.1-9, 2022.
- [9] M. Savic, Y. Ma, G. Ramponi, W. Du, and Y. Peng, Lung Nodule Segmentation with a Region-Based Fast Marching Method, *Sensors (Basel)*, vol. 21, no. 5, pp. 1–32, Mar. 2021, doi: 10.3390/S21051908.
- [10] Choudhury, Avishek, and Sunanda Perumalla. "Detecting breast cancer using artificial Intelligence: CNN", *Technology and Health Care*, Vol 29, Issue no. 1, pp. 33-43,2021.
- [11] Neal Joshua E. S, Bhattacharyya D, Chakravarthy M, and Byun Y. C, 3D CNN with visual insights for early detection of lung cancer using gradient weighted class, *Activation, Journal of Healthcare Engineering*, pp. 1-13, 2021.
- [12] Lakshmanaprabu S. K, Santhosh K, and Balasubramanian P, Optimal deep learning model for classification of lung cancer on CT images using LDA and MGSA, *Journal of Ambient Intelligence and Humanized Computing*, Vol. 10, Issue no 4, pp. 1403-1414, 2019.
- [13] Lu Y, Liang H, Shi S, Fu X, Lung Cancer Detection using a Dilated CNN with VGG16, *4th International Conference on Signal Processing and Machine Learning*, pp45-51, 2021.
- [14] Sannasi Chakravarthy, Rajaguru V, Chaotic crow search algorithm-based feature selection for lung cancer classification, *Biomedical Research*, Vol 30, Issue No.4, pp 774-782, 2019.

- [15] S Bhatia, Y Sinha, L Goel, Lung Cancer Detection: a deep learning approach, *Soft Computing for Problem Solving*, pp 699-705, Springer, Singapore, 2019.
- [16] P. Joon, S. B. Bajaj, and A. Jatain, "Segmentation and detection of lung cancer using image processing and clustering techniques," *Advanced Computing and Intelligent Engineering*, pp. 13–23, Springer, Singapore, 2019.
- [17] A. Masood et al., Computer-Assisted Decision Support System in Pulmonary Cancer detection and stage classification on CT images, *Journal of Biomedical Informatics*, vol. 79, pp. 117–128, Mar. 2018, doi: 10.1016/J.JBI.2018.01.005.
- [18] S. Govindarajan and R. Swaminathan, Differentiation of COVID-19 conditions in planar chest radiographs using optimized convolutional neural networks, *Applied Intelligence*, vol. 51, no. 5, pp. 2764–2775, May 2021, doi: 10.1007/S10489-020-01941-8.
- [19] E. Shelhamer, J. Long, and T. Darrell, Fully Convolutional Networks for Semantic Segmentation, *IEEE Trans Pattern Anal Mach Intelligence*, vol. 39, no. 4, pp. 640–651, Apr. 2017, doi: 10.1109/TPAMI.2016.2572683.
- [20] F. Christ et al., Automatic liver and lesion segmentation in CT using cascaded fully convolutional neural networks and 3D conditional random fields, *Lecture Notes in Computer Science (including subseries Lecture Notes in Artificial Intelligence and Lecture Notes in Bioinformatics)*, vol. 9901 LNCS, pp. 415–423, 2016, doi: 10.1007/978-3-319-46723-8\_48.
- [21] Reddy, T.P.K., Bharathi, P.S. Lung cancer detection using novel residual unity AlexNet-based optimized mish dropout-deep convolutional neural network, *Soft Computer*, 2023. <https://doi.org/10.1007/s00500-023-08970-8>.
- [22] Mesut Togarcar, Burhan Ergen, Zafer Comert, Detection of lung cancer on chest CT images using minimum redundancy maximum relevance feature selection method with convolutional neural networks, *Biocybernetics and biomedical engineering*, vol. 40, no.1, pp. 23-39, March 2020.
- [23] Dhasny Lydia, Prakash M, Performance Evaluation of convolutional neural Network for Lung Cancer Detection, *International Conference on Electronic Systems, and Intelligent Computing (ICESIC)*, April 2022.
- [24] Christian Garbin, Xingquan Zhu, Oge Marques, Dropout vs. batch normalization: an empirical study of their impact to deep learning, *Multimedia Tools and Applications*, January 2020.
- [25] Hidenori Ide, Takio Kurita, Improvement of learning for CNN with ReLU activation by sparse regularization, *International Joint Conference on Neural Networks (IJCNN)*, May 2017, doi: 10.1109/IJCNN.2017.7966185.
- [26] Dhasny Lydia, Prakash M, Performance Evaluation of convolutional neural Network for Lung Cancer Detection, *International Conference on Electronic Systems and Intelligent Computing (ICESIC)*, April 2022, doi 10.1109/ICESIC53714.2022.9783533.
- [27] Da Nóbrega, R.V.M Rebouças Filho, P.P Rodrigues, M.B da Silva, S.P.P, urado Júnior, C.M.J.M, de Albuquerque, V.H.C, "Lung nodule malignancy classification in chest computed tomography images using transfer learning and convolutional neural networks", *Neural Computer*. pp. 11065–11082,2020.
- [28] M. Masud, N. Sikder, A. A. Nahid, A. K. Bairagi, M. A. AlZain, A machine learning approach to diagnosing lung and colon cancer using a deep learning-based classification framework, *Sensors*, vol. 21, no. 3, p. 748, 2021.
- [29] Muhammad Aminu, Noor Atinah Ahmad, Mohd Halim Mohd Noor, Covid-19 detection via deep neural network and occlusion sensitivity maps, *Journal of Healthcare Engineering*, Vol 60, pp. 4829-4855, 2021.
- [30] X. Wang, L. Wang, and P. Zheng, SC-Dynamic R-CNN: A Self-Calibrated Dynamic R-CNN Model for Lung Cancer Lesion Detection, *Computational and Mathematical Methods Medicine*, vol. 2022, 2022, doi: 10.1155/2022/9452157.
- [31] N. S. Nadkarni and S. Borkar, Detection of lung cancer in CT images using image processing, *Proceedings of the International Conference on Trends in Electronics, and Informatics, ICOEI 2019*, vol. 2019-April, pp. 863–866, Apr. 2019, doi: 10.1109/ICOEI.2019.8862577.